

Temperature-based zoning of the Bordeaux wine region.

Benjamin Bois, Daniel Joly, Hervé Quénol, Philippe Pieri, Jean-Pierre Gaudillère, Dominique Guyon, Etienne Saur, Cornelis van Leeuwen

▶ **To cite this version:**

Benjamin Bois, Daniel Joly, Hervé Quénol, Philippe Pieri, Jean-Pierre Gaudillère, et al.. Temperature-based zoning of the Bordeaux wine region.. OENO One, 2018, 52 (4), pp.291-306. 10.20870/oeno-one.2018.52.4.1580 . hal-02056427

HAL Id: hal-02056427
https://hal.science/hal-02056427

Submitted on 26 May 2020

HAL is a multi-disciplinary open access archive for the deposit and dissemination of scientific research documents, whether they are published or not. The documents may come from teaching and research institutions in France or abroad, or from public or private research centers.

L'archive ouverte pluridisciplinaire **HAL**, est destinée au dépôt et à la diffusion de documents scientifiques de niveau recherche, publiés ou non, émanant des établissements d'enseignement et de recherche français ou étrangers, des laboratoires publics ou privés.



Distributed under a Creative Commons Attribution - NonCommercial 4.0 International License

OENO One
VINE AND WINE OPEN ACCESS JOURNAL
Volume 52 > Number 4 > 2018

Temperature-based zoning of the Bordeaux wine region

Benjamin Bois[1,2*], Daniel Joly[3], Hervé Quenol[4], Philippe Pieri[5], Jean-Pierre Gaudillère[5], Dominique Guyon[6], Etienne Saur[7] and Cornelis van Leeuwen[5,8]

Biogéosciences UMR 6282 CNRS / Université Bourgogne Franche Comté, 6 boulevard Gabriel, 21000 Dijon, France
[2]Institut Universitaire de la Vigne et du Vin, 1 rue Claude Ladrey, 21000 Dijon, France
[3]TheMA UMR 6049 CNRS / Université Bourgogne France Comté, France
[4]Laboratoire COSTEL, LETG, UMR 6554 CNRS, Université Rennes 2, Place Recteur Henri le Moal, 35043 Rennes, France
[5]INRA, ISVV, UMR 1287, F-33140 Villenave d'Ornon, France
[6]INRA, UR 1263 EPHYSE, F-33140 Villenave d'Ornon, France
[7]IAVFF-Agreenium, 42 rue Scheffer, 75116 Paris, France
[8]EGFV, Bordeaux Sciences Agro, INRA, Univ. Bordeaux, 33882 Villenave d'Ornon, France

Abstract

Temperature is a driving climate variable for grapevine development and grape ripening kinetics. The current study first reports interpolation of daily minimum and maximum temperature data by a weather station network from 2001 to 2005 in the Bordeaux (France) winegrowing region by means of regression kriging using terrain, satellite and land-cover derived covariates. Second it analyses the interpolation procedure errors in agroclimatic indices by means of cross validation and then it compares the field observations of grapevine phenology to temperature-based predicted phenology applied to interpolated data. Finally it proposes a simple method to perform a zoning of Bordeaux vineyards based upon the spatialized prediction of the day on which grape sugar content reaches 200 $g.L^{-1}$. The zoning performed shows large potential differences in grape maturity date (up to 20 days) induced by temperature spatial variability in a low relief area.

Keywords: Bordeaux wine region, viticultural zoning, grapevine phenology, regression kriging, temperature

Received 1st November 2016 ; Accepted : 24 September 2018 ; Published : 13 December 2018
doi : 10.20870/oeno-one.2018.52.4.1580

*Corresponding author : benjamin.bois@u-bourgogne.fr

OENO One, 2018, **52**, 4, 291-306
©Université de Bordeaux (Bordeaux, France)

Introduction

Climate is one of the most important viticultural variables affecting grapevine development and the enological potential of grapes (van Leeuwen *et al., 20*04). Air temperature, in particular, plays an essential role in the kinetics of vine growth (Buttrose, 1969 ; Buttrose and Hale, 1973 ; Pouget, 1988), timing of phenology (Parker *et al.*, 2013) and grape ripening (Spayd *et al.*, *20*02; Downey *et al.*, *20*06).

The climatic characterization of winegrowing regions relies heavily on air temperature, as evidenced by the significant amount of literature on the subject (Amerine and Winkler, 1944; Gladstones, 1992; White *et al.*, 2006; Bois, 2007; Jones *et al.*, 2009; Jones *et al.*, *20*10). Most spatial analyses of temperature are mainly performed using point data, that is, weather stations (see, for example, Gladstones, 1992; Tonietto and Carbonneau, 2004), or gridded data at 1-km resolution or more (Jones *et al.*, 2009; Jones *et al.*, 2010). Such resolutions are relevant for small spatial and temporal scale zoning (macroclimatic characterization, monthly time steps). However, they do not consider local variations in temperature, which may lead to significant differences in the physicochemical composition of the grapes (Neethling *et al.*, 2011).

The fine-scale analysis of temperature fields can be achieved through three different methods. The first uses a very fine network of temperature sensors that allows sampling at nearly all topographical positions of the study site. This is made possible through the development of automated temperature monitoring devices (electronic sensors/data loggers, many examples are shown in Quénol, 2014). The spatial extent of such monitoring networks is, however, limited by the financial and human costs associated with equipment purchase, installation and maintenance. Furthermore, the development of these networks is relatively new and access to historical data is often limited. The second method – which may be complementary to the first one – estimates temperature fields using meso-scale temperature data (typically a network of weather stations). Such interpolation of spatial data at any point in space is based on spatial statistics, possibly with the use of ancillary variables (environmental covariates), which affects the spatial structure of the temperature fields. The ancillary variables can be collected with a denser, or even systematic, sampling scheme. A typical example is the use of a digital terrain model (DTM) whose topographical descriptors (elevation, slope, orientation, etc.) are often highly correlated with temperature. Temperature is then derived from regression models established between the environmental covariates and station data (Jarvis and Stuart, 2001; Joly *et al.*, 2003; Pape *et al.*, 2009). The third method simulates temperature fields using high-resolution dynamic climate models (Bonnardot and Cautenet, 2009). For the moment, the use of these very high-resolution models requires significant computer resources, and hence long calculation times, thus limiting the extent of climate simulations, both spatially and temporally.

The aim of the present study is to perform a high-resolution (50 m) characterization of thermal diversity in the Gironde vineyards – a region with little relief – and to assess the impact of temperature variations on vine development and grape ripening. The impact of thermal spatial variability on grapevine biology is evaluated by applying phenological models to daily interpolated temperature fields. Phenological stage predictions are tested against data collected on *Vitis vinifera* L. cv. Merlot vine plots. Finally, the 37 AOCs (*appellation areas*) of the Bordeaux wine region are characterized based on the date on which grape sugar content potentially reaches 200 $g.L^{-1}$ (as estimated from interpolated temperature data).

Data and methods

1. Study area

The Bordeaux wine region is located in southwestern France, in the Gironde Department, 20 to 150 km inland from the Atlantic Ocean, between 44.5° and 45.5°N. The vineyards are planted on a wide range of soils, including sand/gravel over Quaternary alluvial deposits, clay over Oligocene calcareous soils, etc. (Wilbert, 1987). According to the Köppen-Geiger classification system, the region, having a warm temperate climate with moderate summers and no dry season (Peel *et al.*, 2007), belongs to the "Cfb" type. From a viticultural perspective, it has been characterized as sub-humid temperate with cool nights (Tonietto and Carbonneau, 2004). Its proximity to the Atlantic Ocean reduces the risk of extreme temperatures (frost or severe heat) for grapevines (Bois *et al.*, 2012).

The Bordeaux wine region is composed of 37 AOCs and covers approx. 240 000 ha, of which approx. 112 600 ha were planted with vines in 2014 (France Agrimer, 2015). The region extends over a large strip along the Gironde estuary and over nearly all the eastern part of the Gironde Department (Figure 1a). Here, five winegrowing regions are represented: Médoc (including Margaux, Saint-Julien, Pauillac and Saint-Estèphe appellations), Graves (including Pessac-Léognan and Sauternes), Entre-Deux-Mers,

©Université de Bordeaux (Bordeaux, France)

Libournais (including Saint-Emilion and Pomerol), and Blayais-Bourgeais. The AOC areas were delineated using the AOC geographical database provided by the Conseil Interprofessionnel du Vin de Bordeaux and the Institut National de l'Origine et de la Qualité.

The surface area covered by AOC regions (238 531 ha) largely exceeds the actual vine planted area (123200 ha in 2005 and 112 600 ha in 2014; France Agrimer, 2015). Furthermore, the delineation of the AOC regions includes built-up areas (urban areas, road networks, etc.) and water bodies, which clearly have no present or future use for vine growing. These non-arable lands were identified using the CORINE Land Cover 2006 geographical database (CLC2006; Büttner *et al.*, 2007). They represent 8332 ha of built-up areas (classes 100 to 142 of CLC2006) and 256 ha of water areas (water streams, water bodies, and part of the estuary; classes CLC2006 500 and above).

Our climate analysis was performed on arable AOC areas (i.e. excluding the *lost* areas). The vector layer of AOC areas was converted to grid format (raster), at 50-m resolution, on a grid identical to that of the digital elevation model (DEM) used for temperature interpolation (BD ALTI, ©IGN). This conversion led to a raster image of 912 418 pixels, corresponding to 228 104 ha, which is slightly below (1839 ha less) the total arable AOC area calculated from the vector layers.

2. Temperature data

This study used daily temperature records (minimum and maximum) collected through the DEMETER and Meteo-France networks of CIMEL automated weather stations over the 2001-2005 period (totaling 1826 days; Figure 1b). In that period, the number of stations increased from 32 (in 2001) to 68 (from 2003 to 2005). The collected data were thoroughly checked by graphically comparing the temporal dynamics of temperatures by groups of 5 to 10 stations. Several types of outliers were detected (database errors using previous years' data; one-day time lag in data series; growing gap in data collected at one station versus surrounding stations, most likely due to sensor drift; sudden gaps of several degrees that lasted for several days); overall, 221 series (of 1 to 1461 daily data each, 4565 values at total) were discarded. This represents 2.3% of the original dataset.

3. Spatial interpolation of temperature

Four methods for spatial interpolation of meteorological data were preliminarily evaluated: the nearest neighbor (NN) method, also known as

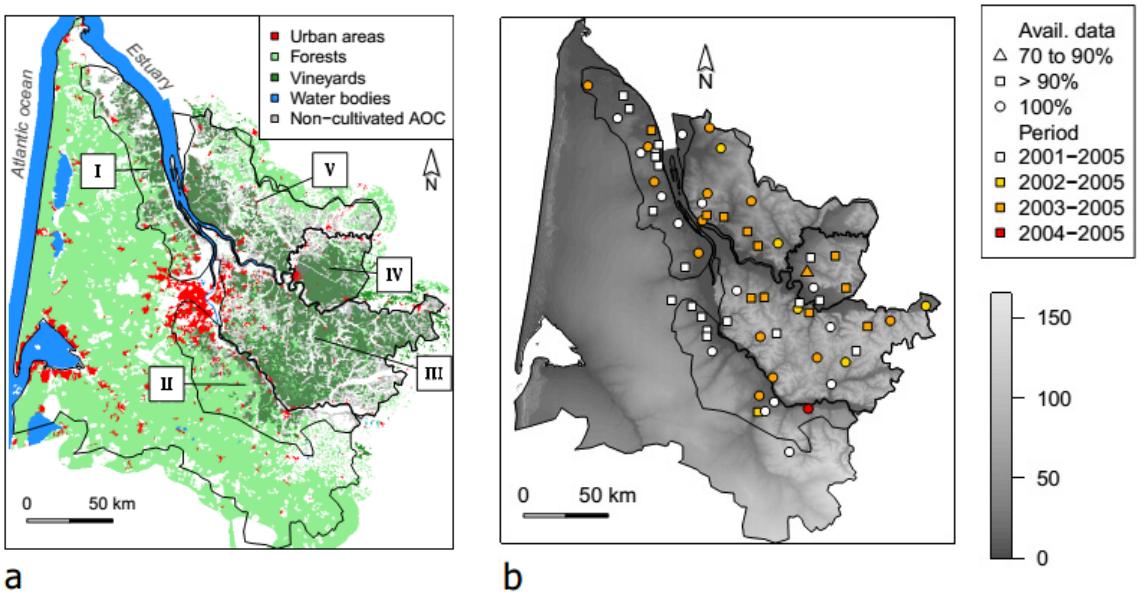


Figure 1. a: Geographical map of Gironde (main land uses, as reported by CORINE Land Cover, 2006; Büttner et al., 2007). The administrative border of the Gironde Department is delineated by a thin black line; the five winegrowing regions of Bordeaux are delineated by a thick black line: I: Médoc; II: Graves and Sauternais; III: Entre-Deux-Mers; IV: Libournais; V: Blayais-Bourgeais. b: Spatial distribution of the weather stations. The sampling period is indicated by colors; the percentage of data available for the 2001-2005 sampling period (after removal of erroneous data and outliers) is indicated by symbols. Elevation (BD ALTI, ©IGN) is indicated by different background shades.

OENO One, 2018, **52**, 4, 291-306
©Université de Bordeaux (Bordeaux, France)

Thiessen polygons (Thiessen, 1911), the ordinary kriging (OK) method (Matheron, 1970), the multiple linear regression (MLR) method, and the regression-kriging (RK) method (Odeha *et al.*, 1994), an approach (equivalent to kriging with external drift) widely used in climatology (Holdaway, 1996; Agnew and Palutikof, 2000; Boer *et al.*, 2001; Stahl *et al.*, 2006; Joly *et al.*, 2010; Hengl *et al.*, 2012). The principle of these techniques is well documented in the literature (for more details, see Cressie, 1993; Wackernagel, 2003).

RK and MLR methods were performed using ancillary data, herein called "environmental covariates". They consisted in a set of rasters (i.e. grids) at 50-m resolution derived from two sources: a 50-m digital elevation model (already mentioned above) from which several geomorphological rasters have been derived (according to Joly *et al.*, 2012) and a Normalized Difference Vegetation Index (NDVI) derived from a Landsat 7 ETM+ satellite image (Chander *et al.*, 2009). Following a preliminary benchmark of the methods, RK, clearly performing more efficiently, was retained.

This preliminary comparison of interpolation methods, as well as a full description of environmental covariates used in regression-based interpolation methods are detailed in supplementary material (SM1).

Temperature interpolation validation set was elaborated by means of Leave-One-Out Cross Validation (LOOCV): an interpolation model was built, for each day, using the set of observed temperature data at *n* stations and withholding the data of one of the *n* stations. The interpolation was performed at the excluded station coordinates, providing an independent comparison between observed and interpolated temperature data at that site. This was repeated *n* times, each time with a different weather station (see Stone, 1974, for discussion about cross validation).

The validation dataset obtained was used both to compare the interpolation methods through a preliminary benchmark and to evaluate interpolation error propagation within agroclimatic indices (see Section 5 below).

The performance of temperature and agroclimatic spatialization procedures was evaluated with three statistical indicators, comparing the data recorded at the stations (observations) with interpolated data (predicted values):

- the coefficient of determination (R^2) between observed and predicted values

- the modeling efficiency (EF; Mayer and Butler, 1993), defined as:

$$EF = 1 - \frac{\sum_{i=1}^{n}(P_i - O_i)^2}{\sum_{i=1}^{n}(O_i - \bar{O})^2} \quad (1)$$

- the root mean square error (RMSE), defined as:

$$RMSE = \sqrt{\frac{\sum_{i=1}^{n}(P_i - O_i)^2}{n}} \quad (2)$$

where P_i is the predicted value, O_i is the observed value at station i of the n stations used for LOOCV, and $\bar{O}$ is the mean value of all O_i observations.

4. Phenological observations

A database of phenological observations - mid-flowering date (112 vine plots) and mid-veraison date (32 vine plots) - was compiled for grapevines (*Vitis vinifera* L. cv. Merlot) over the period 2001 to 2005 (Lebaron, 2006), made on commercial vineyards. These were weekly observations collected by three institutions through three grapevine monitoring networks across Gironde: the Faculty of Enology of the University of Bordeaux, the French Institute of Vine and Wine (IFV) and the Gironde Chamber of Agriculture. Observations were made every week, walking through single plots and noting the average stage of the plot by observing inflorescences and grapes. For flowering stage, stages were noted as early flowering, mid-flowering and late flowering. If no mid-flowering was recorded, the mid-flowering stage was determined using linear interpolation between both early and late flowering dates. Veraison was noted similarly, though the approximate percentage of berries having reached veraison was provided for some plots (University of Bordeaux network). The maximum uncertainty of observed data was considered to be 6 days max, and 3.5 days on average. The dataset contained several missing values (data not collected for one or more of the five vintages). Finally, 320 observations for mid-flowering dates (out of 112 plots x 5 vintages = 560 potential data) and 68 for mid-veraison dates (out of 160 potential data) were available.

5. Phenological model and agroclimatic indices

Seven types of daily temperature-based agroclimatic indices were selected:

©Université de Bordeaux (Bordeaux, France)

- The dates of phenological stages and "grape theoretical maturity" for *Vitis vinifera* cv. Merlot, as calculated with the GFV (Grapevine Flowering Veraison) model (Parker *et al., 20*11; Parker, 2012). "Grape theoretical maturity" corresponds to the day on which grape sugar content reaches 200 $g.L^{-1}$ for a specific variety. The GFV model was fitted to grape sugar content data collected in various locations and years (Parker, 2012). The model performance for the cultivar Merlot is 7.98 days (RMSE, see Parker, 2012). Note that grapes are generally harvested at higher sugar levels (220 – 230 $g.L^{-1}$), so the index anticipates real harvest dates by 2 or 3 weeks. However "grape theoretical maturity" modeling remains a relevant tool to compare the delay (in days) between early and late ripening vineyard blocks;

- The number of frost days at the start of the growing season, that is, the number of days with minimum air temperature ≤ -1°C, between March 1 and June 30. This methodology assumes that when shade temperature (at 1.5 or 2 m above ground) has reached -1°C, the vegetation closer to the ground is exposed, in case of temperature inversion, to temperatures close to -3°C, which is the damage threshold for young vine shoots (Fuller and Telli, 1999);

- The number of "high heat" days, that is, the number of days with shade maximum air temperature ³ 35°C, between June 1 and September 30. It is hypothesized that temperatures above 35°C induce a thermal stress for grapevine, limiting grape anthocyanin content and significantly disturbing berry sugar accumulation (Sepulveda and Kliewer, 1986; Mori *et al.,* 2007). Above 40°C, photosynthetic activity is also impaired (Luo *et al.,* 2011);

- The mean minimum temperature for the month of September, called the "Cool night Index" (CNI; Tonietto and Carbonneau, 2004). This index reflects the positive influence of cool night-time temperatures during the ripening period on grape secondary metabolite content (Kliewer and Torres, 1972; Tonietto and Carbonneau, 2004; Mori *et al.*, 2005). Note that the reference period to calculate CNI is not relevant for warm vintages such as 2003 in Bordeaux, where maturation took place mostly during August and harvest was performed early September. We however stuck to this reference period in order to respect the calculation standards of this index;

- The minimum, maximum and mean daily temperature averages from April to September, the growing season period in Bordeaux, from budburst to harvest. Jones (2006) also considers the month of October. It was discarded here, as harvest rarely occurs during October in the Bordeaux wine region.

The GFV model is based on the sum of daily average temperatures above a base temperature (i.e. above 0°C), starting from the 60th day of year (DOY 60; March 1 or February 29). The dates of mid-flowering, mid-veraison and 200 $g.L^{-1}$ grape sugar content are obtained when thermal summation reaches threshold values (called *F**), as defined for each grape variety. The model was developed and validated using a large database of phenological observations and grape ripening monitoring for the 1952-2010 period, representing data for over 81 grape varieties in several countries, including France, Spain, Italy, Greece and Switzerland (Parker *et al.*, 2011; Parker, 2012). It was used here to estimate the dates of these two phenological stages and the date on which grape sugar content reaches 200 $g.L^{-1}$ (used as proxy for maturity) for Merlot grapevines (Table 1).

Results and discussion

1. Validation of interpolated agroclimatic indices

Considering the performance of the four interpolation methods (see SM1), temperature estimations have been calculated using RK in any point of the study area (i.e. 50-m resolution DEM grid located within the Bordeaux winegrowing region). To assess daily interpolation error propagation within agroclimatic indices mapping, RK cross validation data were used

Table 1. GFV model parameters and associated uncertainties for Merlot grapevines (Parker *et al.*, 2011; Parker 2012).

	Threshold value (*F**, °C)	RMSE (days)
Mid-flowering DOY	1 266	4.24
Mid-veraison DOY	2 627	1.75
"200 $g.L^{-1}$ sugars" DOY	3 165	7.89

RMSE = root mean square error; DOY = day of year

OENO One, 2018, **52**, 4, 291-306
©Université de Bordeaux (Bordeaux, France)

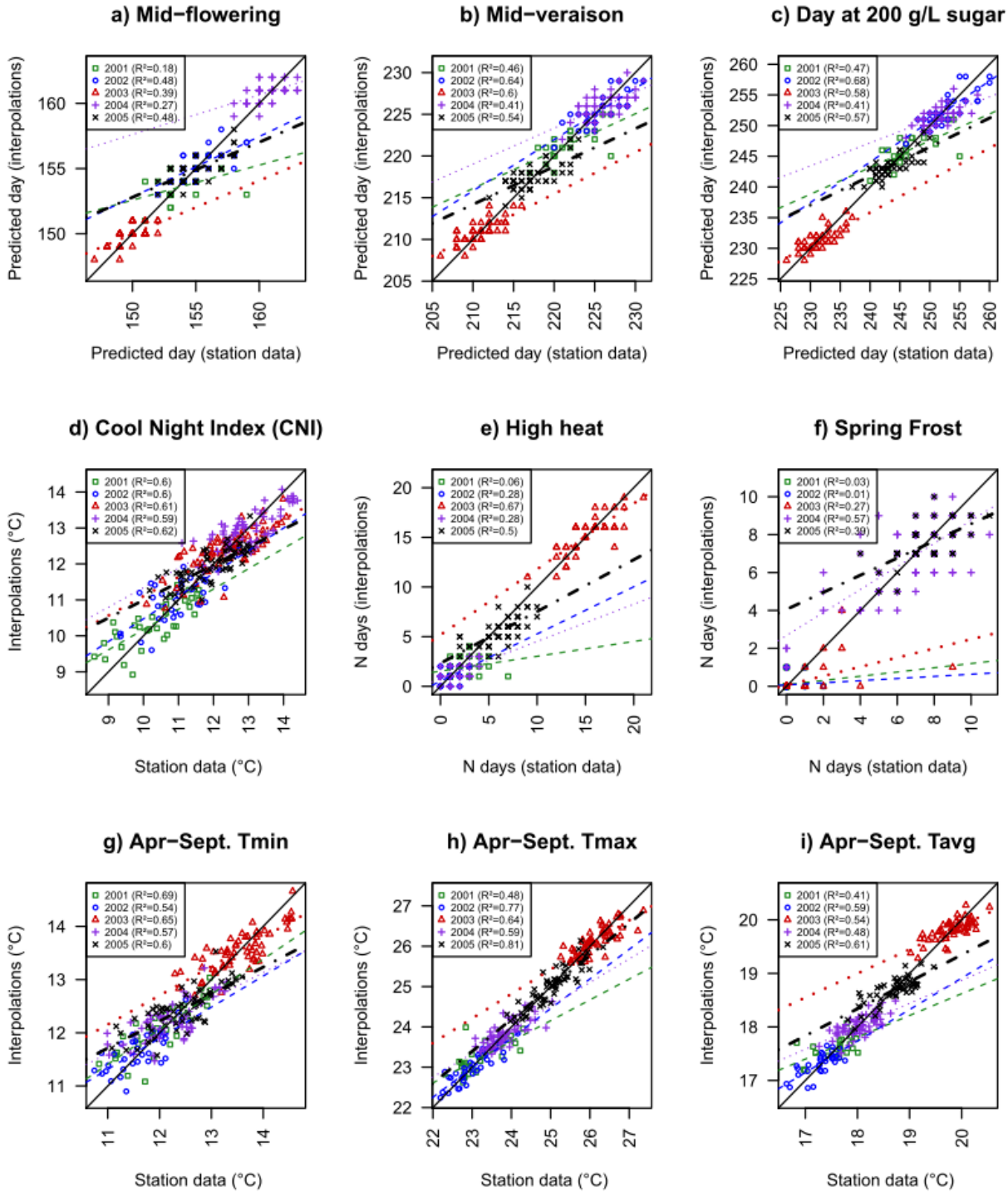


Figure 2. Regressions between modeled phenological stages / calculated agroclimatic indices using data from each weather station and modeled phenological stages / calculated agroclimatic indices using data from daily temperatures interpolated by RK (cross validation). a, b and c: day of year of the occurrence of phenological stages and on which grape sugar content reaches 200 g.L^{-1} (theoretical maturity); d: cool night index (°C); e: number of high heat days; f: number of spring frost days; g, h and i: Means of minimum, maximum and average dailytemperature during the growing season (April to September).

©Université de Bordeaux (Bordeaux, France)

to calculate several agroclimatic indices: mid-flowering date, mid-veraison date and day on which berry sugar content reaches 200 $g.L^{-1}$ (used as proxy for maturity), as estimated by the GFV model for the Merlot cultivar; the CNI index; the number of frost days (in the spring) and high heat days (in the summer); and minimum, maximum and mean daily temperature averages from April to September. This analysis was restricted to the RK method because of its better fit to observed daily temperature fields over the other interpolation methods.

The agroclimatic indices calculated from daily interpolated Tmin and Tmax data were, in general, close to observed station data (Figure 2). The spatial variability between and within years was well represented, with the exception of mid-flowering dates in 2001 and 2004 and the low number of high heat days in 2001, 2002 and 2004, which showed a poorer fit ($R^2 \leq 0.28$; Figures 2a and 2e). The number of spring frost days was the only index to exhibit an overall poor fit (Figure 2f). Mid-flowering dates were relatively close to one another, such that differences of one or two days significantly reduced the R^2 values. Regarding high heat days (number of days with Tmax ³ 35°C), RK interpolation allowed a fairly good representation of spatial variability, especially in years with frequent high temperature days (2003 and 2005). Similarly, the spatial interpolation of spring frost days (number of days with Tmin ≤ -1°C) improved with increasing frequency (2004 and 2005, with up to 11 frost days between March and June). By contrast, the EF values for spring frosts were negative in 2001 and 2002, when the number of frost days stayed below 2 (data not shown). The spatial variability of CNI was fairly well represented (R^2 ranging from 0.59 to 0.62), as those of the minimum (R^2 ranging from 0.54 to 0.69, Figure 2g) and mean (R^2 ranging from 0.41 to 0.61, Figure 2i) daily temperatures averaged from the whole grapevine growing season, i.e. April to September. The more accurate interpolations were achieved for the daily maximum temperature averages on the same period (R^2 ranging from 0.48 to 0.81, Figure 2h). Interpolation by RK tended to lower the spatial variability of predicted phenological stages or agroclimatic indices, as reflected by the regression slopes for each vintage (< 1): values predicted from spatial interpolation were under (over)estimated at stations with high (low) observed values (Figure 2).

We compared the relevance of using the IC approach (Interpolate then Calculate), i.e. daily interpolation of temperature data to perform agroclimatic indices, rather than first calculating these indices and then interpolating the results (i.e. the CI approach: Calculate then Interpolate). As shown in Figure 3, interpolating first (IC) provided most of the time a higher efficiency than spatial interpolation of the indices (CI). For the yearly number of frost and heat

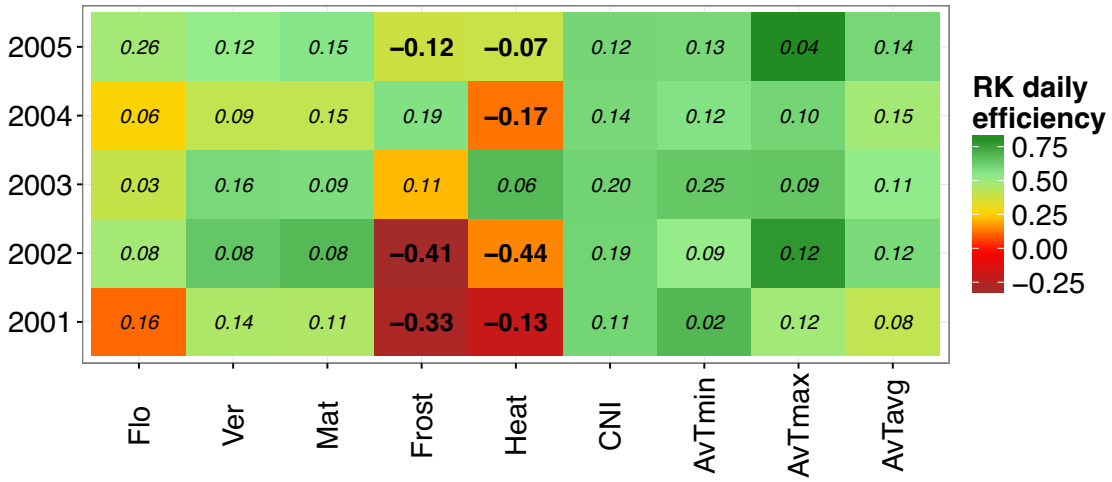


Figure 3. Heatmap of the agroclimatic indices spatialization efficiency (based on LOOCV results) using minimum and maximum daily temperature regression kriging. The figures indicate the efficiency difference IC – CI, i.e. the difference between this regression kriging procedure (interpolating first and then calculating the agroclimatic indices, IC) and the one that calculates first agroclimatic indices and then interpolates the results using regression kriging (calculate then interpolate, CI). Negative figure, in bold, indicates cases for which CI > IC. Flo: mid-flowering day, Ver: mid- veraison day, Mat: theoretical maturity day (200 $g.L^{-1}$ of sugar), Frost: number of spring frost days, Heat: number of high heat days, CNI: cool night index, AvTmin, AvTmax and AvTavg: minimum, maximum and mean temperature averages from April to September. Flo, Ver and Mat are calculated using the GFV heat summation model. See text for additional information.

OENO One, 2018, **52**, 4, 291-306
©Université de Bordeaux (Bordeaux, France)

days, however, calculating first then interpolating clearly provided more accurate spatialization, especially for years during which these heat/frost days where absent or rare (i.e. spring frost days and heat days during 2002, Figure 3). These indices are very sensitive to daily temperature spatial interpolation errors. Interpolation generated values beyond the lower (upper) thresholds for heat (frost) days event.

Results previously obtained when comparing both approaches diverge, so that no approach could be initially preferred. When mapping soil characteristics, Stein *et al.* (1991) systematically obtained lower mean squared errors (MSE) using universal (co-)kriging with CI, while Bosma *et al.* (1994) had lower MSE with IC using ordinary kriging, but CI and IC differences became nil when the sample size was high (N = 200 and more). Sinowski *et al.* (1997) obtained more accurate prediction in soil water properties estimates when preferring IC. Mardikis *et al.* (2005) observed little differences when comparing both approaches to calculate the Penman-Monteith reference evapotranspiration.

The dates of occurrence of phenological stages predicted by the GFV model were calculated from daily temperature data estimated at the coordinates of Merlot vine plots for which mid-flowering and mi-veraison dates were available (phenological database from the monitoring networks of the Gironde Chamber of Agriculture, the Faculty of Enology of Bordeaux, and the IFV; see paragraph 2 of the Data & Methods section above). The comparison of predicted (GFV model applied to spatialized temperatures) and observed data is shown in Figure 4.

The estimation of mid-flowering and mid-veraison dates was consistent with observations from year to year. However, the spatial performance (within vintages) of the prediction of mid-flowering dates was mediocre: the percentage of explained variance (R^2) did not exceed 36%. Furthermore, the year-to-year variability of the timing of this stage was highly underestimated. We propose two hypotheses to explain this poor result. First, on the one hand, the spatial interpolation underestimates the spatial variability (in Figure 4a, slopes of linear regression models of predicted values as function of observed values are below 1); on the other hand, the GFV model tends to under (over)estimate the timing of the late (early) phenological stages (Parker *et al.*, 2011). Both of these errors, smoothing space and time variability, cumulate to reduce strongly the quality of mid-flowering estimates. Second, one has to consider that flowering is a phenological stage that occurs rapidly (within less than a week), and which observation is much less precise than mid-veraison for red cultivars. Consequently, additional uncertainty concerning mid-flowering observations on *Vitis vinifera* cv. Merlot here might contribute to the strong

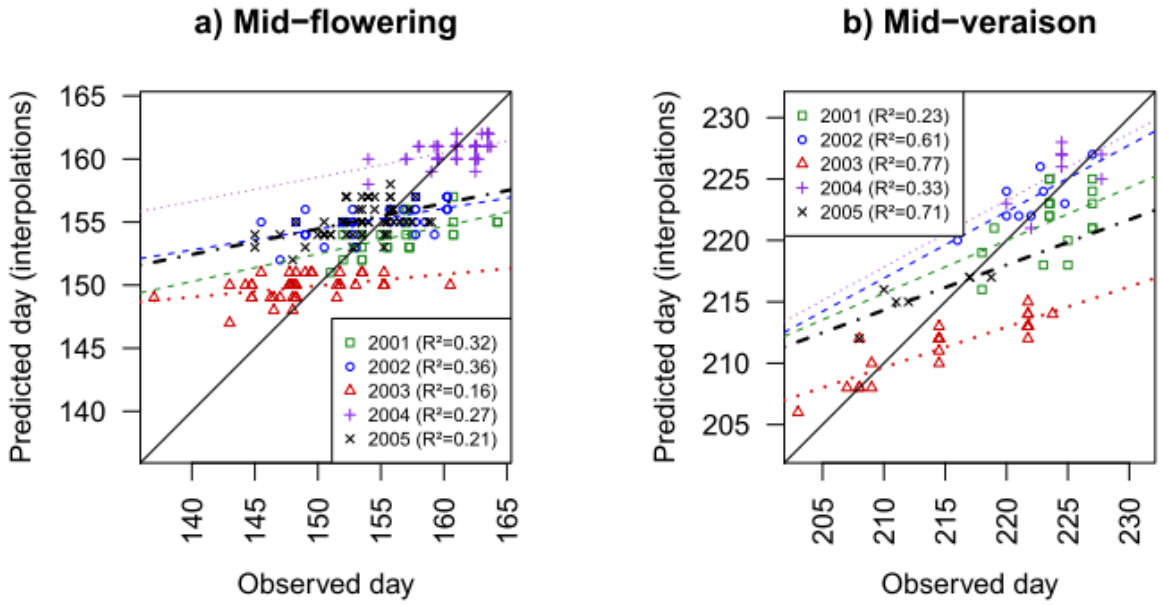


Figure 4. Regressions between observed phenological stages (day of year) and phenological stages predicted from the GFV model applied to daily temperatures interpolated by RK at the coordinates of Merlot vine plots. a: mid-flowering; b: mid-veraison.

©Université de Bordeaux (Bordeaux, France)

difference between temperature-based spatialized flowering and field observations.

The predicted mid-veraison dates also tended to underestimate the spatial variability but to a lesser extent. However, the spatialized predictions of the date of occurrence of this phenological stage were much closer to observations, explaining up to 77% of the variance in observed dates in 2003.

2. Agroclimatic zoning of the Gironde wine region

As RK daily interpolation error propagation was limited within agroclimatic indices mapping, this spatialization procedure was considered reliable enough to be used for the spatialization of agroclimatic indicators relevant to viticulture in Gironde.

The day on which grape sugar content reaches 200 $g.L^{-1}$ (GFV model), hereafter referred to as "theoretical maturity", was chosen to characterize the thermal potential of Gironde vineyards. The time of theoretical maturity was calculated for 912 418 pixels (50-m resolution) within Gironde AOCs (total area of 228 104 ha), for each of the five years of the study period (2001-2005), using the interpolated daily Tmin and Tmax data. This maturity-based zoning was performed as follows: (i) for each vintage, the estimated maturity days were classified into five equal interval classes: pixels with the earliest potential maturity (earliest day of year) were assigned a value of 1 and the latest a value of 5. (ii) The year-to-year standard deviation in class values was calculated for each pixel. Pixels with a standard deviation > 1 took on a class 6 value ("unstable"). A large standard deviation indeed indicates that the relative ranking of such pixel varies significantly from one year to another, thereby preventing its precise ranking (early vs. late area). (iii) The final ranking of the pixels that remained relatively consistent from year to year (standard deviation ≤ 1) was obtained by averaging the class values (values from 1 to 5) over the 5-year study period (rounded to the nearest integer). As a result, six potential maturity classes were obtained: "very early" (=1), "early" (=2), "intermediate" (=3), "late" (=4), "very late" (=5) and "unstable" (=6).

Year-to-year variation in ranking was low for much of the study area and only 18 ha (i.e. 0.01% of the Bordeaux AOC areas) was classified as "unstable".

Table 2 shows the average potential day of theoretical maturity (expressed in day of year) for each class. Differences of 2 to 4 days were observed between classes, with a maximum of 20 days between the "earliest" and "latest" pixels (2001). Standard deviations varied from 0.6 to 1.6 days between classes (excluding the "unstable" class), which is slightly below the RMSE obtained for cross validation (1.6 to 2.9 days). Increasing the number of classes for zoning is therefore not useful, given the uncertainties associated with spatialization.

Table 2. Average (Avg.) and standard deviation (s) of the "sugar content = 200 $g.L^{-1}$" day of year for each maturity class. Average difference ([Avg.]) corresponds to the difference between "very late" and "very early" averages. Maximum difference ([Max.]) corresponds to the difference between the two extreme days of year across the 912 418 pixels (50-m resolution) within the study area. Real harvest generally takes place two or three weeks later, at sugar levels of 220 to 230 $g.L^{-1}$

		Day of year of "theoretical maturity" (sugar content = 200 g.L-1) for each class							
	Year	Very early	Early	Intermediate	Late	Very late	Unstable	[Avg.]	[Max.]
	2001	242	245	248	251	255	247	14	20
	2002	248	251	253	257	260	253	12	16
Avg.	2003	228	230	232	234	236	234	8	11
	2004	248	250	252	254	256	254	8	12
	2005	240	242	243	246	248	246	8	15
	2001	0.8	1.3	1.6	1.5	1.5	3.4		
	2002	1.0	1.1	1.3	1.2	0.9	0.7		
s	2003	0.8	0.6	0.8	0.7	0.6	1.5		
	2004	0.7	0.7	0.8	0.8	0.8	1.5		
	2005	1.0	0.6	0.9	0.9	1.2	1.4		

OENO One, 2018, **52**, 4, 291-306
©Université de Bordeaux (Bordeaux, France)

The great majority of the pixels within Bordeaux AOC areas belonged to the "intermediate" class (69.1% of the total area; Table 3 and Figure 5). The "very early" and "early" areas were found along the Garonne and Dordogne valleys, in Haut-Médoc (region I), on the Garonne River's left (region II) and right banks (region III), in the Libournais (region IV), and within the Canon Fronsac appellation (region V). The entire Pomerol appellation (region IV) was classified as "very early" (3%) and "early" (97%). A substantial part of the Saint-Emilion and Pessac-Léognan appellations (7%) was classified as "very early". In the Médoc, Pauillac, Saint-Julien, Margaux and Saint-Estèphe were classified as "early" or "intermediate", while the rest of this area was mainly classified as "intermediate" to "late" This is consistent with empirical knowledge of the Bordeaux wine region.

The areas classified as "late" and "very late" were found in the northwestern part of Médoc (region I) as well as in the northeastern part of the Bordeaux wine region (region IV and region V).

The spatial zoning based upon temperature can be viewed as the result of two combinatory, but different spatial structures of minimum and maximum temperatures during the grapevine growing season (Figure 6). April to September minimum temperature 5-year average ranges from 10.3°C (Sauternes area, region II) to 13.15°C (Pessac-Léognan, within the city of Pessac, region II). The lowest minimum temperature values are found in the southwestern part of region II as well as in the Dordogne plain close to Saint-Emilion (region IV) and in the most western (eastern) parts of region I (IV). The highest minimum temperatures during the growing season are found in Pauillac, Saint-Julien and Saint-Estèphe villages (east-central part of region I) as well as in areas close to the city of Bordeaux (Pessac-Léognan, region II), in the Côtes de Bourg area (southwestern part of region V) and on the Pomerol/Saint-Emilion plateau (region IV). April to September 2001-2005 maximum temperature ranges from 22.65°C (the northern part of the Côtes de Blaye area, region V) to 24.6 °C (Sauternes area, region II). The high maximum temperatures are mostly found in the Dordogne and Garonne valleys (region II, south of region IV). Low maximum temperatures are found in the northern part of Médoc (region I) and Côtes de Blaye (region V) areas.

The zoning shown in Figure 5 can be used as a relevant tool for vineyard management. Selecting the grape variety according to the temperature potential of the area is crucial for ensuring proper grape ripeness. The two main grape varieties grown in the Bordeaux region are Merlot and Cabernet-Sauvignon. The former reaches maturity 7 to 15 days earlier than

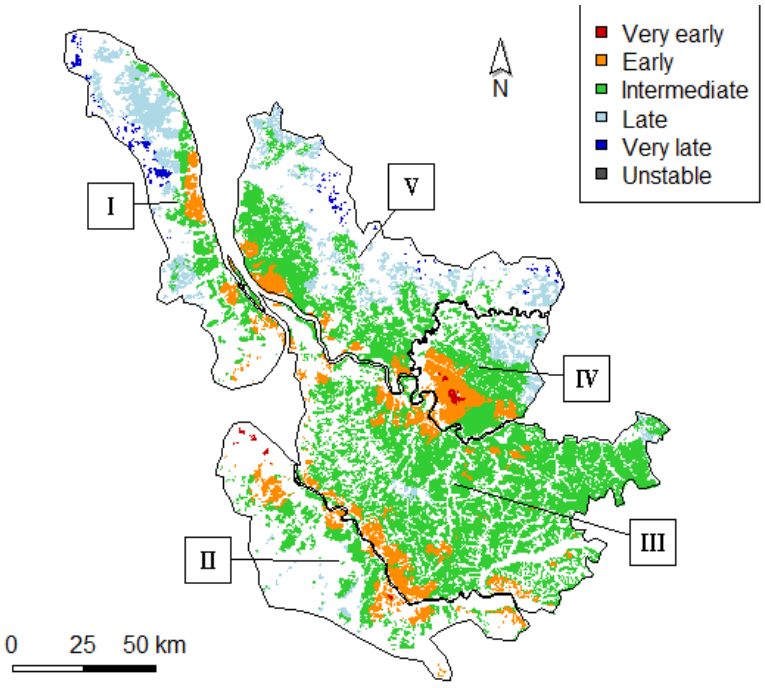


Figure 5. Temperature-based zoning of grape "theoretical maturity" (sugar content = 200 g.L^{-1}) in the five wine regions of Bordeaux: I: Médoc (including Margaux, Saint-Julien, Pauillac and Saint-Estèphe); II: Graves and Sauternais (including Pessac-Léognan); III: Entre-Deux-Mers; IV: Libournais (including Saint-Emilion and Pomerol); V: Blayais-Bourgeais.

©Université de Bordeaux (Bordeaux, France)

Table 3. Percentage of the total area of each Gironde's AOC in the different maturity potential classes. Regions: I: Médoc; II: Graves and Sauternais; III: Entre-deux-Mers; IV: Libournais; V: Blayais-Bourgeais; others: islands of the Gironde estuary

Region	AOC	Very early	Early	Intermediate	Late	Very late	Unstable	Area (ha)
I	Bordeaux - Bordeaux Supérieur	0	39	59	2	0	0	1 440
	Haut-Médoc	0	6	54	31	9	0	8 108
	Listrac	0	0	29	71	0	0	1 363
	Margaux	0	37	63	0	0	0	1 772
	Médoc	0	0	8	81	11	0	10 113
	Moulis	0	0	39	61	0	0	1 007
	Pauillac	0	79	21	0	0	0	1 543
	Saint-Estèphe	0	30	61	9	0	0	1 538
	Saint- Julien	0	59	41	0	0	0	997
II	Barsac	0	20	80	0	0	0	835
	Bordeaux - Bordeaux Supérieur	0	38	61	1	0	0	2 993
	Cerons, Graves - Graves Supérieures	0	6	85	9	0	0	2 137
	Graves - Graves Supérieures	0	19	69	12	0	0	7 798
	Pessac-Léognan	7	47	46	0	0	0	3 701
	Sauternes	2	47	50	1	0	0	2 104
III	Premières Côtes de Bordeaux	0	25	75	0	0	0	3 681
	Premières Côtes de Bordeaux, Cadillac	0	44	56	0	0	0	8 202
	Bordeaux - Bordeaux Supérieur	0	32	68	0	0	0	4 269
	Côtes de Bordeaux, Saint-Macaire	0	18	82	0	0	0	4 485
	Entre-deux-Mers	0	8	92	0	0	0	57 667
	Entre-deux-Mers Bordeaux, Haut-Benauge	0	9	85	6	0	0	6 772
	Graves de Vayres	0	75	25	0	0	0	1 276
	Loupiac	0	77	23	0	0	0	818
	Sainte-Croix-du-Mont	0	83	17	0	0	0	760
	Saint-Foy Bordeaux	0	0	96	4	0	0	16 133
IV	Bordeaux - Bordeaux Supérieur	0	6	68	26	0	0	6 992
	Bordeaux, Côtes de Francs	0	0	42	58	0	0	1 012
	Côtes de Castillon	0	19	64	17	0	0	5 475
	Lalande de Pomerol	0	64	36	0	0	0	1 377
	Lussac Saint-Emilion	0	0	61	38	0	1	1 820
	Montagne Saint-Emilion	0	8	91	1	0	0	2 097
	Pomerol	3	97	0	0	0	0	901
	Puisseguin Saint-Emilion	0	0	95	5	0	0	1 041
	Saint-Emilion	7	64	30	0	‡	0	6 855
	Saint-Georges Saint-Emilion	0	19	81	0	0	0	274
V	Premières Côtes de Blaye, Côtes de Blaye	0	4	68	28	0	0	16 665
	Blaye - Blaye area	0	0	27	49	24	0	2 403
	Bordeaux - Bordeaux Supérieur	0	4	66	27	2	0	20 631
	Canon Fronsac	0	76	24	0	0	0	396
	Côtes de Bourg	0	30	64	6	0	0	6 829
	Fronsac	0	23	77	0	0	0	1 305
Others	Bordeaux - Bordeaux Supérieur	0	19	81	0	0	0	523
	Total	0.3	15.7	69.1	13.6	1.3	0.0	228 104

OENO One, 2018, **52**, 4, 291-306
©Université de Bordeaux (Bordeaux, France)

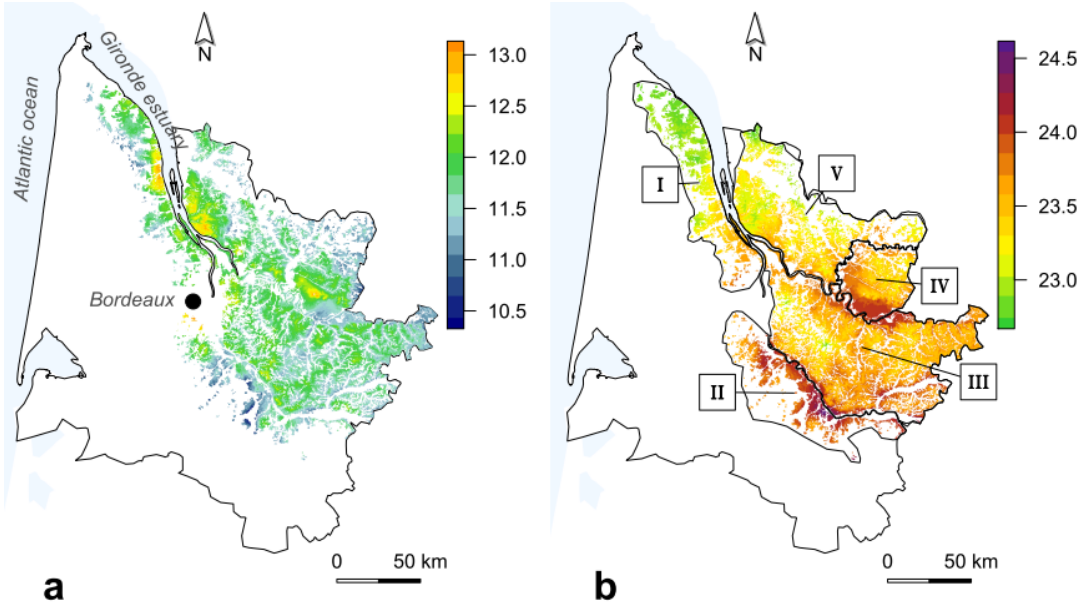


Figure 6. April to September daily minimum (a) and maximum (b) temperature (°C) averages from 2001 to 2005.

the latter. Cabernet-Sauvignon is traditionally grown in Médoc (region I), a region that showed a wide range of temperature potentials. The grape ripening process is most likely to be negatively affected in the cooler west and north parts of the region, especially in late vintages. The use of Merlot, however, could help to obtain more consistent ripeness in this part of the Médoc. On the other hand, the projected temperature increase for the 21st century (IPCC, 2014) may promote the ripening of Cabernet-Sauvignon, including in the "latest" ripening areas of Gironde. As for Merlot, it is traditionally grown in the Saint-Emilion and Pomerol region, one of the "earliest" maturity potential (temperature) areas. Increasing the proportion of Cabernet franc (a grapevine variety with intermediate earliness in comparison to Merlot and Cabernet-Sauvignon) and Cabernet-Sauvignon in that region could reduce the risk of over-ripeness (too high sugar levels in grapes resulting in excessive alcohol in wines; cooked fruit aromas; lack of acidity and freshness in wines) in the decades to come.

Amongst the five vintages for which spatial temperature variability has been analyzed in this study, years 2003 and 2005 exhibit both substantially dryer (-208 and -197 mm in cumulated rainfall) and warmer (+2.3 and +1.7°C in average temperature) growing season conditions, when compared to 1981-2010 averages (Figure 7). Summer warmth and precipitation deficit in 2003 could be considered as typical to what is expected in the late 21st century in Switzerland and nearby countries such as France (Schär *et al.*, 2003). In the Bordeaux wine region, the spatial ranges in minimum and maximum temperature (April to September 2001-2005 averages) are 2.85°C and 1.95°C, respectively (Figure 6). This spatial variation is close to expected rise in temperature throughout the 21st century (scenarios and multi-models median between +2 and +3°C in southwestern France, compared to the 1986-2005 average, as shown in the regional atlases in IPCC 2014). Our results are consistent with previous studies which have shown large spatial variation in temperature at local scale (see for instance Quénol, 2014 and Le Roux *et al.*, 2017). They confirm that (1) the impact of climate change differs in a consistent manner in space and (2) adaptation to climate change does not necessarily imply a long range shift in vineyard location towards higher latitudes or altitudes, as cool areas for vine production can be found within the same wine producing region.

Using interpolated temperature data for zoning viticultural potentialities has already been performed in many researches (see for instance section 3.4 in the review by Vaudour *et al., 20*15). In most cases, interpolation and agroclimatic models error propagation are not considered. Therefore, it is impossible to confirm if the expected spatial variability of the crop response to climate, as depicted by the zoning procedure, is effective. At meso-scale level, a few studies (such as Failla *et al.*, 2004 or Madelin and Beltrando, 2005) have compared the spatial potentialities of climate for grapevine

©Université de Bordeaux (Bordeaux, France)

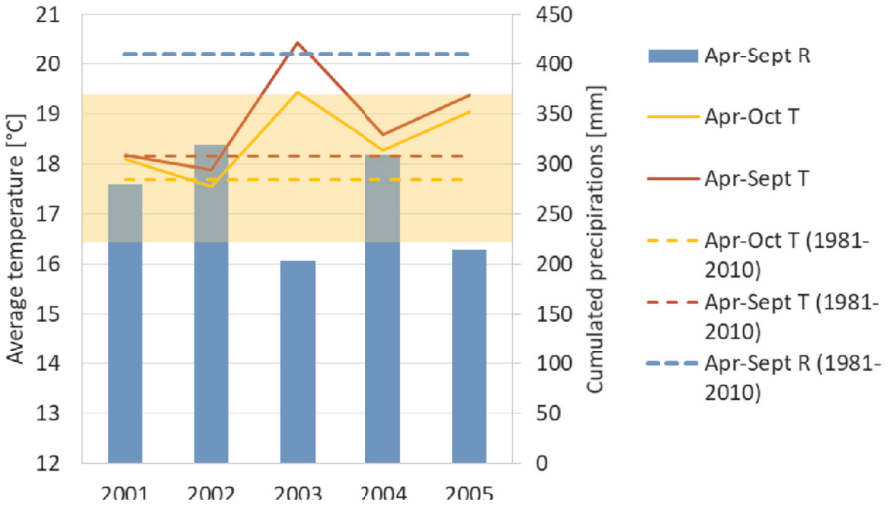


Figure 7. 2001 to 2005 vintages growing season temperatures and precipitations in Bordeaux. Apr-Sept R = April to September precipitation [mm]; Apr-Oct T = April to October average temperature (i.e. Jones' average growing season temperature, Jones 2006) [°C]; Apr-Sept T = April to September average temperature [°C]. The full lines and the vertical bars represent data for each of the years 2001 to 2005. The dotted lines represent climate normals (1981-2010 averages). The orange transparent stripe corresponds to the "optimum" Apr-Oct T range for Cabernet-Sauvignon proposed by Jones (2006). Data collected from the reference weather station of Bordeaux Merignac airport (44°49'50°N; 0°41'29»W). Source: Meteo-France.

production by means of field observations. Our study has shown, using field observations, that despite a series of uncertainties or errors cumulated throughout the potential grapevine phenological spatialization procedure (phenological model errors, climate stations location representativeness, spatial interpolation errors, timing and accuracy of phenological observations in the field), an acceptable prediction of grapevine mid-veraison spatial variability could be achieved at meso-scale level.

Conclusions

In this work, we presented a comprehensive approach to zoning of agroclimatic potential using spatially interpolated daily temperature data.

The extent of interpolation errors within agroclimatic indices calculated each year based on daily temperature interpolations is limited. These indices were therefore used for the spatialization of the dates of two phenological stages in *Vitis vinifera* cv. Merlot, a grape variety largely grown in Gironde. The phenological timing predicted by a thermal summation model using spatial temperature trends could not reproduce the spatial variability of the mid-flowering date observed within a vine plot. By contrast, the predicted spatial mid-veraison date was consistent with vine plot observations.

A 5-class spatial characterization of the Bordeaux wine region using theoretical maturity (day on which grape sugar content reaches 200 $g.L^{-1}$), predicted by cumulated degree-days (GFV model), as an indicator of the impact of spatial climate variability on grape ripening is presented. The high repeatability of the spatial distribution of temperature fields implied high reliability in zoning. Average differences of approximately 10 days were observed over the entire study area. Because our interpolation method underestimates spatial variability in temperatures, real differences in the day when grapes reach full ripeness are likely to be even greater. Such meso-scale climatic differences over a wine producing region with little relief can have a significant impact on the enological potential of the grapes. In light of these results, spatial variability in temperatures should be considered as an integrated component of an appellation's natural terroir factors. Our results can help growers to optimize wine quality by adapting plant material (grapevine variety and root-stock) as well as present and future management practices to spatial temperature variability.

Acknowledgements : The authors thank Stéphanie Lebaron for her meticulous work in compiling the phenological database, and the IFV (Marc Raynal), the Gironde Chamber of Agriculture (Laurent Bernos and Jean-Philippe Gervais) and the Faculty of Enology of Bordeaux (Laurence Geny) for kind

OENO One, 2018, **52**, 4, 291-306
©Université de Bordeaux (Bordeaux, France)

cooperation. This work was supported by the Conseil Interprofessionnel du Vin de Bordeaux.

References

Agnew M.D. and Palutikof J.P., 2000. GIS-based construction of baseline climatologies for the Mediterranean using terrain variables. Clim Res 14:115–127. doi:10.3354/cr014115

Amerine M.A. and Winkler A.J., 1944. Composition and quality of musts and wines of California grapes. Hilgardia 15:493–673. doi:10.3733/hilg.v15n06p493

Boer E.P.J., de Beurs K.M. and Hartkamp A.D., 2001. Kriging and thin plate splines for mapping climate variables. Int J Appl Earth Obs Geoinf 3:146–154. doi:10.1016/S0303-2434(01)85006-6

Bois B., 2007. Cartographie agroclimatique à méso-échelle : méthodologie et application à la variabilité spatiale du climat en Gironde viticole. Conséquences pour le développement de la vigne et la maturation du raisin. PhD thesis, University of Bordeaux (France).

Bois B., Blais A., Moriondo M. and Jones G.V., 2012. High resolution climate spatial analysis of European winegrowing regions. In: Proc IXth International Terroir Congress. Dijon - Reims (France), pp. 217–220.

Bonnardot V. and Cautenet S., 2009. Mesoscale atmospheric modeling using a high horizontal grid resolution over a complex coastal terrain and a wine region of South Africa. J Appl Meteorol Climatol 48:330–348. doi:10.1175/2008JAMC1710.1

Bosma W.J.P., Marinussen M.P.J.C. and van der Zee SEAT M., 1994. Simulation and areal interpolation of reactive solute transport. Geoderma 62:217–231. doi:10.1016/0016-7061(94)90037-X

Büttner G., Soukup T. and Sousa A., 2007. CLC2006 technical guidelines (technical report no. 17/2007). European Environment Agency, Luxembourg.

Buttrose M.S., 1969. F Vegetative growth of grapevine varieties under controlled temperature and light intensity. Vitis 8:280-285. doi:10.1086/336487

Buttrose M.S. and Hale C.R., 1973. Effect of temperature on development of the grapevine inflorescence after bud burst. Am J Enol Vitic 24:14–16.

Chander G., Markham B.L. and Helder D.L., 2009. Summary of current radiometric calibration coefficients for Landsat MSS, TM, ETM+, and EO-1 ALI sensors. Remote Sens Environ 113:893–903. doi:10.1016/j.rse.2009.01.007

Cressie N., 1993. Statistics for Spatial Data, Revised Edition. Wiley, New York.

Downey M.O., Dokoozlian N.K. and Krstic M.P., 2006. Cultural practice and environmental impacts on the flavonoid composition of grapes and wine: a review of recent research. Am J Enol Vitic 57:257–268. http://www.ajevonline.org/content/ajev/57/3/257.full.pdf

Failla O., Mariani L., Brancadoro L., Minelli R., Scienza A., Murada G. and Mancini S., 2004. Spatial distribution of solar radiation and its effects on vine phenology and grape ripening in an alpine environment. Am J Enol Vitic 55:128–138.

France Agrimer, 2015. Les chiffres de la filière viti-vinicole : données statistiques 2004/2014. France Agrimer, Montreuil-Sous-Bois (France).

Fuller M.P. and Telli G., 1999. An investigation of the frost hardiness of grapevine (*Vitis vinifera*) during bud break. Ann Appl Biol 135:589–595. doi:10.1111/j.1744-7348.1999.tb00891.x

Gladstones J., 1992. Viticulture and Environment. Winetitles, Underdale, South Australia.

Hengl T., Heuvelink G.B.M., Tadić M.P. and Pebesma E.J., 2012. Spatio-temporal prediction of daily temperatures using time-series of MODIS LST images. Theor Appl Climatol 107:265–277. doi:10.1007/s00704-011-0464-2

Holdaway M.R., 1996. Spatial modeling and interpolation of monthly temperature using kriging. Clim Res 6:215–225. doi:10.3354/cr006215

IPCC., 2014. Climate Change 2013: The Physical Science Basis: Working Group I Contribution to the Fifth Assessment Report of the Intergovernmental Panel on Climate Change. Cambridge University Press. Cambridge, United Kingdom and New York, NY, USA.

Jarvis C.H. and Stuart N., 2001. A comparison among strategies for interpolating maximum and minimum daily air temperatures. Part II: the interaction between number of guiding variables and the type of interpolation method. J Appl Meteorol 40:1075–1084. doi:10.1175/1520-0450(2001)040<1075:ACASFI>2.0.CO;2

Joly D., Nilsen L., Fury R., Elvebakk A. and Brossard T., 2003. Temperature interpolation at a large scale: test on a small area in Svalbard. Int J Climatol 23:1637–1654. doi:10.1002/joc.949

Joly D., Nilsen L., Brossard T. and Elvebakk A., 2010. Plants as bioindicator for temperature interpolation purposes: analyzing spatial correlation between botany based index of thermophily and integrated temperature characteristics. Ecol Indic 10:990–998. doi:10.1016/j.ecolind.2010.02.007

Joly D., Bois B. and Zaksek K., 2012. Rank-ordering of topographic variables correlated with temperature. Atmos Clim Sci 2:139–147. doi:10.4236/acs.2012.22015

Jones G.V., 2006. Climate and terroir: impacts of climate variability and change on wine. In: Macqueen RW, Meinert LD (eds). Fine Wine and Terroir - The Geoscience Perspective. Geological Association of Canada, St. John's, Newfoundland, 247 pp.

©Université de Bordeaux (Bordeaux, France)

Jones G.V., Moriondo M., Bois B., Hall A. and Duff A., 2009. Analysis of the spatial climate structure in viticulture regions worldwide. Bull OIV 82:507–517.

Jones G.V., Duff A.A., Hall A. and Myers J.W., 2010. Spatial analysis of climate in winegrape growing regions in the Western United States. Am J Enol Vitic 61:313–326.

Kliewer W.M. and Torres R.E., 1972. Effect of controlled day and night temperatures on grape coloration. Am J Enol Vitic 23:71–77.

Lebaron S., 2006. Étude de la variabilité spatio-temporelle des stades phénologiques et de la maturation du raisin en Gironde viticole. Dissertation, ENITA Bordeaux (France).

Le Roux R., de Rességuier L., Corpetti T., Jégou N., Madelin M., van Leeuwen C. and Quénol H., 2017) Comparison of two fine scale spatial models for mapping temperatures inside winegrowing areas. Agric For Meteorol 247:159–169. doi:10.1016/j.agrformet.2017.07.020

Luo H.-B., Ma L., Xi H.-F., Duan W., Li S.-H., Loescher W., Wang J.-F. and Wang L.-J., 2011. Photosynthetic responses to heat treatments at different temperatures and following recovery in grapevine (*Vitis amurensis* L.) leaves. PLoS ONE 6:e23033. doi:10.1371/ journal.pone.0023033

Madelin M. and Beltrando G., 2005. Spatial interpolation-based mapping of the spring frost hazard in the Champagne vineyards. Meteorol Appl 12:51–56. doi:10.1017/S1350482705001568

Mardikis M.G., Kalivas D.P. and Kollias V.J., 2005. Comparison of interpolation methods for the prediction of reference evapotranspiration—an application in Greece. Water Resour Manage 19:251–278. doi:10.1007/s11269-005-3179-2

Matheron G., 1970. La théorie des variables régionalisées et ses applications. Cahiers du Centre de Morphologie Mathématique de Fontainebleau, fascicule 5, Paris.

Mayer D.G. and Butler D.G., 1993. Statistical validation. Ecol Model 68:21–32. doi:10.1016/0304-3800(93)90105-2

Mori K., Saito H., Goto-Yamamoto N., Kitayama M., Kobayashi S, Sugaya S, Gemma H and Hashizume K., 2005. Effects of abscisic acid treatment and night temperatures on anthocyanin composition in Pinot noir grapes. Vitis 44:161–165. https://www.vitis-vea.de/admin/volltext/e051824.pdf

Mori K., Goto-Yamamoto N., Kitayama M. and Hashizume K., 2007. Loss of anthocyanins in red-wine grape under high temperature. J Exp Bot 58:1935–1945. doi:10.1093/jxb/erm055

Neethling E, Barbeau G, Quénol H and Bonnefoy C., 2011. Évolution du climat et de la composition des raisins des principaux cépages cultivés dans le Val de Loire. Climatologie 8:77–90. doi:10.4267/climatologie.323

Odeha IOA, McBratney AB and Chittleborough DJ., 1994. Spatial prediction of soil properties from landform attributes derived from a digital elevation model. Geoderma 63:197–214. doi:10.1016/0016-7061(94)90063-9

Pape R., Wundram D. and Löffler J., 2009. Modelling near-surface temperature conditions in high mountain environments: an appraisal. Clim Res 39:99–109. doi:10.3354/cr00795

Parker A.K., 2012. Modelling phenology and maturation of the grapevine *Vitis vinifera* L.: varietal differences and the role of leaf area to fruit weight ratio manipulations. PhD thesis, Lincoln University, New-Zealand. http://dspace.lincoln.ac.nz/bitstream/handle/10182/5635/Parker_PhD.pdf?sequence=3

Parker A.K, Garcia de Cortázar-Atauri I., van Leeuwen C. and Chuine I., 2011. General phenological model to characterise the timing of flowering and veraison of *Vitis vinifera* L. Aust J Grape Wine Res 17:206–216. doi:10.1111/j.1755-0238.2011.00140.x

Parker A.K., Garcia de Cortázar-Atauri I., Chuine I, Barbeau G., Bois B., Boursiquot J.-M., Cahurel J.-Y., Claverie M., Dufourcq T., Gény L., Guimberteau G., Hofmann R., Jacquet O., Lacombe T., Monamy C., Ojeda H., Panigai L., Payan J.-C., Rodriquez-Lovelle B., Rouchaud E., Schneider C., Spring J.-L., Storchi P., Tomasi D., Trambouze W., Trought M. and van Leeuwen C., 2013. Classification of varieties for their timing of flowering and veraison using a modeling approach. A case study for the grapevine species *Vitis vinifera* L. Agric For Meteorol 180:249–264. doi:10.1016/j.agrformet.2013.06.005

Peel M.C., Finlayson B.L. and McMahon T.A., 2007. Updated world map of the Köppen-Geiger climate classification. Hydrol Earth Syst Sci 11:1633–1644. doi:10.5194/hess-11-1633-2007

Pouget R., 1988. Le débourrement des bourgeons de la vigne : méthode de prévision et principes d'établissement d'une échelle de précocité de débourrement. Conn Vigne Vin 22:105–123. doi:10.20870/oeno-one.1988.22.2.1260

Quénol H., 2014. Changement Climatique et Terroirs Viticoles. Eds. Lavoisier, Paris.

Schär C., Vidale P.L., Lüthi D., Frei C., Häberli C., Liniger M.A. and Appenzeller C., 2004. The role of increasing temperature variability in European summer heatwaves. Nature 427:332–336. doi:10.1038/nature02300

Sepulveda G. and Kliewer W.M., 1986. Effect of high temperature on grapevines (*Vitis vinifera* L.). II. Distribution of soluble sugars. Am J Enol Vitic 37:20–25.

Sinowski W., Scheinost A.C. and Auerswald K., 1997. Regionalization of soil water retention curves in a

©Université de Bordeaux (Bordeaux, France)

highly variable soilscape, II. Comparison of regionalization procedures using a pedotransfer function. Geoderma 78:145–159. doi:10.1016/S0016- 7061(97)00047-5

Spayd S.E., Tarara J.M., Mee D.L. and Ferguson J.C., 2002. Separation of sunlight and temperature effects on the composition of *Vitis vinifera* cv. Merlot berries. Am J Enol Vitic 53:171–182.

Stahl K., Moore R.D., Floyer J.A., Asplin M.G. and McKendry I.G., 2006. Comparison of approaches for spatial interpolation of daily air temperature in a large region with complex topography and highly variable station density. Agric For Meteorol 139:224–236. doi:10.1016/j.agrformet.2006.07.004

Stein A., Staritsky I.G., Bouma J., Van Eijnsbergen A.C. and Bregt A.K., 1991. Simulation of moisture deficits and areal interpolation by universal cokriging. Water Resour Res 27:1963–1973. doi:10.1029/91WR00505

Stone M., 1974. Cross-validatory choice and assessment of statistical predictions. J R Stat Soc Series B Stat Methodol 36:111–147. https://www.jstor.org/stable/2984809

Thiessen A.H., 1911. Precipitation averages for large areas. Mon Wea Rev 39:1082–1089. doi:10.1175/1520-0493(1911)39<1082b:PAFLA> 2.0.CO;2

Tonietto J. and Carbonneau A., 2004. A multicriteria climatic classification system for grape-growing regions worldwide. Agric For Meteorol 124:81–97. doi:10.1016/j.agrformet.2003.06.001

van Leeuwen C., Friant P., Choné X., Tregoat O., Koundouras S. and Dubourdieu D., 2004. Influence of climate, soil, and cultivar on terroir. Am J Enol Vitic 55:207–217.

Vaudour E., Costantini E., Jones G.V. and Mocali S., 2015. An overview of the recent approaches to terroir functional modelling, footprinting and zoning. SOIL 1:287–312. doi:10.5194/soil-1-287-2015

Wackernagel H., 2003. Multivariate Geostatistics: An Introduction with Applications, 3rd ed. Springer-Verlag, Berlin. doi:10.1007/978-3-662-05294-5

White M.A., Diffenbaugh N.S., Jones G.V., Pal J.S. and Giorgi F., 2006. Extreme heat reduces and shifts United States premium wine production in the 21st century. Proc Natl Acad Sci USA 103:11217–11222. doi:10.1073/pnas.0603230103

Wilbert J., 1987. La pédologie en Aquitaine - cartographie et inventaire. CRAA-INRA (France).

©Université de Bordeaux (Bordeaux, France)